Human Reproduction, pp. 1–13, 2023
https://doi.org/10.1093/humrep/dead013

human reproduction

ORIGINAL ARTICLE *Infertility*

Impact of first chemotherapy exposure on follicle activation and survival in human cryopreserved ovarian tissue

Melody Devos [1], Paula Diaz Vidal[1], Jason Bouziotis[2], Ellen Anckaert[3], Marie-Madeleine Dolmans [4,5], and Isabelle Demeestere [1,6,*]

[1]Research Laboratory on Human Reproduction, Université Libre de Bruxelles (ULB), Brussels, Belgium [2]Department of Biomedical Research, HUB-Hopital Erasme, Université Libre de Bruxelles, Brussels, Belgium [3]Follicle Biology Laboratory, Vrije Universiteit Brussel (VUB) and Universitair Ziekenhuis Brussel (UZ Brussel), Jette, Belgium [4]Gynecology Department, Cliniques Universitaires St-Luc, Brussels, Belgium [5]Gynecology Research Laboratory, Institut de Recherche Expérimentale et Clinique, Université Catholique de Louvain, Brussels, Belgium [6]Gynecology and Obstetrics Department, Fertility Clinic, HUB-Erasme Hospital, Université Libre de Bruxelles, Brussels, Belgium

*Correspondence address. Research Laboratory on Human Reproduction, Université Libre de Bruxelles, Campus Erasme CP636, 808 Route de Lennik, 1070 Brussels, Belgium. E-mail: isabelle.demeestere@ulb.be https://orcid.org/0000-0002-3192-6565

Submitted on June 8, 2022; resubmitted on December 30, 2022; editorial decision on January 17, 2023

STUDY QUESTION: Does chemotherapy exposure prior to ovarian tissue cryopreservation (OTC) impact the signaling pathways governing follicle activation and survival for prepubertal and postpubertal patients?

SUMMARY ANSWER: Chemotherapy exposure prior OTC increases follicle apoptosis rates but not follicular activation, although the PI3K/AKT/mTOR and Hippo signaling pathways were modified in the cortex.

WHAT IS KNOWN ALREADY: OTC is currently the only available fertility preservation procedure for children and for patients who have already started their treatment. While previous studies have not observed harmful impacts of first chemotherapy exposure on OTC outcomes, the consequences of treatment on follicle activation and survival need to be further investigated. To address this question, we evaluated signaling pathway modifications induced by chemotherapy exposure according to pubertal status.

STUDY DESIGN, SIZE, DURATION: Cryopreserved ovarian tissues from postpubertal (12–29 years old, n = 8) and prepubertal (3–10 years old, n = 8) cancer patients donated for research were thawed and cultured for 24 h. Analyses of the survival of the follicles and stroma, and of the PI3K/AKT/mTOR and Hippo signaling pathways, were conducted at thawing and after culture. Ovarian fragments exposed to chemotherapy before collection were compared to non-exposed controls.

PARTICIPANTS/MATERIALS, SETTING, METHODS: Histological investigations were performed to assess the distribution of the follicles, stroma fibrosis, vessel integrity, and apoptosis levels. It included follicular counting, collagen staining, immunostaining on CD31 and gH2AX, as well as TUNEL staining. To explore follicle activation in the different groups, the PI3K/AKT/mTOR and Hippo signaling pathways were investigated by gene expression analyses of isolated follicles and protein analyses on whole fragments through western blots and immunostaining.

MAIN RESULTS AND THE ROLE OF CHANCE: We first assessed the impact of a first exposure to chemotherapy on the collagen density and vessels in ovarian tissues at thawing and after culture. While no differences in collagen density were observed according to age or previous treatment, the vascularization area (CD31+) was significantly lower in tissue from previously exposed patients compared to non-treated ones. Apoptosis analyses (TUNEL) revealed an acute deleterious impact on follicle survival after chemotherapy exposure without affecting the follicular density. Surprisingly, leukemic patients had a significantly higher percentage of gH2AX-positive follicles, indicating a DNA damage response, compared to the other patients. The proportion of activated follicles appeared to decrease following exposure to chemotherapy, suggesting that it at least did not increase activation process. Stable KIT LIGAND gene and protein expression and cKIT protein levels were observed among the groups, confirming the absence of activation. Analysis of the PI3K pathway did not reveal a difference in the AKT phosphorylation level between the groups, but pRPS6 was significantly higher in tissue from patients previously exposed

© The Author(s) 2023. Published by Oxford University Press on behalf of European Society of Human Reproduction and Embryology. All rights reserved.
For permissions, please email: journals.permissions@oup.com

Downloaded from https://academic.oup.com/humrep/advance-article/doi/10.1093/humrep/dead013/7022048 by Universite Catholique de Louvain user on 08 February 2023

to chemotherapy compared to that from non-exposed patients. Finally, protein and gene analyses on Hippo pathway signaling showed a higher LATS1 protein level in the cortex after chemotherapy exposure.

LIMITATIONS, REASONS FOR CAUTION: The heterogeneity of the human fragments, and the limited number of patients included in the cohort have to be considered as important study limitations. Moreover, this study did not explore the long-term consequences of chemotherapy on follicular development. Therefore, the results should be interpreted with caution.

WIDER IMPLICATIONS OF THE FINDINGS: These results underscore the deleterious effect of previous chemotherapeutic treatment on follicle survival. Although follicular density was not reduced, these data suggested that exposure to chemotherapy impacts follicular apoptosis and the DNA damage response. Chemotherapy-induced activation was not observed despite the impact on mTOR and Hippo signaling pathways in the whole cortex.

STUDY FUNDING/COMPETING INTEREST(S): This work was funded by an Excellence of Science (EOS) Grant (ID: 30443682) and was supported by Fonds Erasme. I.D. and M.-M.D. are associate researchers at Fonds National de la Recherche Scientifique de Belgique (FNRS). There are no competing interests.

TRIAL REGISTRATION NUMBER: N/A.

Key words: ovarian reserve / cryopreservation / chemotherapy / ovarian tissue transplantation / fertility preservation / follicle activation / DNA damage response

Introduction

Improvements in early diagnosis and therapies have remarkably increased the global survival rate of cancer patients, raising awareness of the long-term effects of oncological regimens on quality of life (Dinikina *et al.*, 2021; Filippi *et al.*, 2021). Chemotherapy exposure can damage the ovarian follicular pool and induce acute or late premature ovarian insufficiency (POI) (Lambertini *et al.*, 2020). The deleterious impact of chemotherapy on ovarian function depends on drug type and dose, the combination of different agents, the duration of exposure, and the age of the patient (Chiarelli *et al.*, 1999; Meirow *et al.*, 2010). Alkylating agents, such as cyclophosphamide (CPA), can induce treatment-related amenorrhea in female patients, with a high risk of POI (>80%) for cumulative equivalent doses (CED) >6 g/m^2 (ESHRE Guideline Group on Female Fertility Preservation *et al.*, 2020). In this context, offering fertility preservation counseling to these patients is highly recommended (ESHRE Guideline Group on Female Fertility Preservation *et al.*, 2020; Lambertini *et al.*, 2020; Mulder *et al.*, 2021). Among the available techniques, ovarian tissue cryopreservation (OTC) is recognized as an innovative effective alternative to oocytes freezing and is the only available option for children (Jensen *et al.*, 2016). Ovarian tissue transplantation is effective for restoration of ovarian function using cryopreserved ovarian tissue but cannot be proposed to all patients, especially when malignant cells are potentially involved the ovary. Therefore, the development of alternatives, such as *in vitro* follicle development, is considered to be a research priority but remains poorly effective. Among the limitations of the human follicle culture system, the massive follicular activation that occurs spontaneously *in vitro* and the accelerated follicular growth rates associated with the procedure have raised questions about the quality of the oocytes obtained (McLaughlin *et al.*, 2018). Moreover, OTC is often performed after a first exposure to chemotherapy that may impact the subsequent culture. The harmful effects of chemotherapy exposure concern all ovarian cell types, from the follicle to the stroma and the vessels (Nicosia *et al.*, 1985; Meirow, 2000; Meirow *et al.*, 2007; Spears *et al.*, 2019). Studies in mouse models have revealed induction of apoptosis in growing follicles exposed to CPA and a depletion of primordial follicles (PFs) through massive activation called the 'burn out' effect (Oktem and Oktay, 2007; Kalich-Philosoph *et al.*, 2013; Chen *et al.*, 2016). To date, this activation of PFs after chemotherapy exposure is largely debated (Szymanska *et al.*, 2020).

While the disruption of signaling pathways regulating follicular quiescence has been demonstrated during chemotherapy exposure, direct impacts on the ovarian reserve are less clear (Meirow *et al.*, 2010; Ben-Aharon and Shalgi, 2012; Kano *et al.*, 2017). PF activation is a crucial step of folliculogenesis regulated by two local signaling pathways, the PI3K/AKT/mTOR pathway and the Hippo signaling pathway (Adhikari *et al.*, 2010; Kawamura *et al.*, 2013; Guo and Yu, 2019; Devos *et al.*, 2020; Grosbois *et al.*, 2020). The PI3K pathway is a regulator of cell growth and is activated in the follicle by KIT LIGAND (KL) (Driancourt *et al.*, 2000; Hsueh, 2014). PI3K activity leads to the phosphorylation of protein kinase B (AKT) by the kinase-30-phosphoinositide-dependent kinase 1 (PDK1) and the mechanistic target of rapamycin complex 2 (mTORC2). AKT is a central regulator that phosphorylates several proteins, such as Forkhead box O3 (FOXO3) in the nucleus, inducing the removal of its quiescence activity, and the tuberous sclerosis complex 1/2 (TSC1/2) protein, leading to the activation of mTORC1 (Castrillon, 2003; Manning and Cantley, 2007; Huang *et al.*, 2008; John *et al.*, 2008). In turn, mTORC1 activity leads to activating phosphorylations of ribosomal protein S6 (RPS6) and eukaryotic translation initiation factor 4E (eIF4E), promoting growth (Mamane *et al.*, 2004; Huang *et al.*, 2008; Adhikari *et al.*, 2010).

The Hippo signaling pathway is regulated by the physical environment and cell density. It has been recently shown to be involved in follicle activation, although its physiological role remains poorly understood. Under basal conditions, the core component of this pathway includes the mammalian Ste-20 like kinase 1/2 (MST1/2) and Salvador (SAV1) complex that activates the large tumor suppressor homolog 1/2 (LATS1/2) (Couzens *et al.*, 2017). In turn, LATS1/2 inhibits, by phosphorylation, Yes-associated protein (YAP) and its transcriptional co-activator PDZ-binding motif (TAZ), repressing the expression of growth and survival genes such as Connective growth tissue factor (*CCN*) and Baculoviral IAP repeat containing (*BIRC*) (Zhou *et al.*, 2009; Harvey *et al.*, 2013; Zygulska *et al.*, 2017). The involvement of this pathway in follicle activation was considered after human

Downloaded from https://academic.oup.com/humrep/advance-article/doi/10.1093/humrep/dead013/7022048 by Universite Catholique de Louvain user on 08 February 2023

ovarian processing for cryopreservation (Grosbois *et al.*, 2020; Lunding *et al.*, 2020). Transformation of actin forms in the cortex after fragmentation appears to disrupt the Hippo pathway, leading to an increase in the activity of the YAP/TAZ complex in the nucleus, inducing follicle activation (Kawamura *et al.*, 2013).

In this context, the impact of a first exposure to chemotherapy regimen on the follicular growth and survival of thawed cultured ovarian tissue requires further investigation. This study aimed to evaluate the effects of chemotherapy exposure on follicle activation and survival using a short-term *in vitro* culture system of cryopreserved ovarian tissues from cancer patients.

Materials and methods

Samples

Ovarian cortical biopsies were obtained from 16 cancer patients who underwent OTC: 8 prepubertal and 8 postpubertal patients. The ovarian tissues were cryopreserved using a slow-freezing technique at Erasme or Saint-Luc hospitals (Brussels, Belgium) and stored in liquid nitrogen. All selected patients provided informed written consent to donate their residual frozen tissue to research at the end of the storage period. This project was approved by the Erasme Hospital Ethical Committee (Brussels, Belgium) with reference P2020/401.

Tissue processing

The cortical tissues were thawed according to the Erasme clinical protocol previously described (Demeestere *et al.*, 2003, 2006). Thawed tissue was processed in dissection medium composed of Leibovitz's L-15 Medium (Gibco, Belgium) complemented with 2 mM glutamine (Sigma, Belgium), 2 mM sodium pyruvate (Sigma, Belgium), 3 mg/ml human serum albumin (HSA) (CAF DCF, Belgium), 30 µg/ml penicillin G (Sigma, Belgium), and 50 µg/ml streptomycin sulfate (Sigma, Belgium). The fragment size was homogenized to obtain $4\times2\times0.5\,mm^3$ fragments that were processed for histological, gene or protein expression analyses at thawing or after 24 h of culture. Culture medium was composed of McCoy's 5a modified medium (Gibco, Belgium) supplemented with 25 mM HEPES, 0.1% HSA, 2.5 µg/ml transferrin (Roche, Germany), 4 ng/ml selenium (Sigma, Belgium), 3 mM glutamine, 50 µg/ml ascorbic acid (Sigma, Belgium), 30 µg/ml penicillin G, and 50 µg/ml streptomycin. Fragments were cultured into 300 µl of pH calibrated and pre-warmed culture medium for 24 h at 37 °C in a humidified incubator with 5% CO_2, as previously described (Grosbois and Demeestere, 2018). Overall, 37 homogenized fragments were used for histological analyses (postpubertal = 20; prepubertal = 17/treated = 21; untreated = 16), 38 for gene analyses (postpubertal = 17; prepubertal = 21/treated = 25; untreated = 13), and 69 for western blots (postpubertal = 39; prepubertal = 30/treated = 28; untreated = 41).

Follicle distribution

After fixation in paraformaldehyde 4% for 24 h at 4 °C, the tissues were embedded into 2% agarose, dehydrated in successive ethanol baths, embedded in paraffin, and serially sectioned at 5 µm thickness (five section per series). Slides were then deparaffinized and rehydrated, and the first sections of each series were stained with hematoxylin–phloxin to perform morphological analyses and follicle counting. Only follicles with a visible nucleus were counted to avoid double counting in all sections (24–72 sections per patient and timepoint) and were classified as primordial (single flattened layer of granulosa cells (GCs) around the oocyte), transitory (flattened and cuboidal GCs), primary (single layer of cuboidal GCs) or secondary (more than one layer of cuboidal GCs) stages. PFs were considered as quiescent while the other follicle stages were grouped into the 'activated follicles' group. The follicle distribution is presented as total follicle number per mm^2 (density) and as percentages (number of healthy follicles in each group over the total number of follicles). Each section surface was measured to calculate the follicular density. Atretic follicles were counted separately based on the morphological characteristic (abnormal nucleus, condensation of chromatin and organelles, and asymmetry of the follicle structure), and are reported as the proportion of the total follicle number to calculate the 'atresia rate'.

Apoptosis assay

Follicle death was assessed through staining of DNA fragmentation by TdT-mediated dUTP-biotin nick-end labeling (TUNEL) applying the In Situ Death Cell Detection kit instructions (Roche, Germany). Deparaffined and rehydrated sections were treated with 20 µg/ml proteinase K in 10 mM Tris pH 7.4 (Qiagen, Netherlands), labeled with the kit reagents according to manufacturer instructions, and counterstained with 1 µg/ml Hoechst. Positive and negative controls were obtained by treatment with 50 IU/ml DNAse I (Invitrogen, USA) and enzyme-free buffer solution, respectively. Each follicle containing one positive cell was considered as TUNEL positive. The positive follicles were counted and classified according to their growth stage.

Collagen density assay

To investigate the density of collagen I and III fibers, Sirius Red staining was performed on the slides using the Picro Sirius Red Stain Kit (Abcam, UK). Briefly, the tissue was dehydrated, exposed to Sirius red solution for 1 h, and rinsed with acetic acid 0.5% before dehydration and mounting.

Immunohistology

To evaluate the DNA damage response (DDR), vessel integrity and the expression level of follicle activation signaling pathway components, immunofluorescence staining was performed for gH2AX, CD31, KL, pRPS6, pAKT, and YAP. After rehydration of the sections, epitope retrieval was performed through heat-mediated incubation into citrate buffer (Sigma, Belgium). Non-specific binding sites were saturated using 5% normal goat serum (Vector Laboratories, UK) and the slides were incubated overnight with the primary and the appropriate biotinylated secondary antibodies (listed in Supplementary Table SI). Finally, conjugation with avidin fluorescein (A2001, Vector Laboratories, UK) or Texas Red (A2006, Vector Laboratories, UK) allowed detection of the staining.

Western blot analysis

Tissues were cut into small pieces and mixed in Laemmli buffer solution including protease (ThermoFisher, Belgium) and phosphatase

Downloaded from https://academic.oup.com/humrep/advance-article/doi/10.1093/humrep/dead013/7022048 by Universite Catholique de Louvain user on 08 February 2023

(Roche, Germany) inhibitors using MagNA Lyser instrument (Roche, Germany) as previously described (Grosbois and Demeestere, 2018). Proteins were separated by 5–12% sodium dodecyl sulfate/polyacrylamide gel electrophoresis (SDS/PAGE) before being transferred onto nitrocellulose membranes (Bio-Rad, Belgium). Membranes were exposed to primary antibodies (ACTIN, AKT, cKIT, LATS1, pAKT, pRPS6, pYAP, RPS6, and YAP) at 1:500 overnight at 4 °C and with the correspondent horseradish peroxidase-conjugated secondary antibody for 1 h at room temperature (Supplementary Table SI). The protein bands were detected by exposure to the SuperSignal West Femto Chemiluminescent Substrate (ThermoFisher, Belgium) and observed with ChemiDoc XRS+ System imager (Bio-Rad, Belgium).

Imaging and quantification

Histological sections were observed using a Nikon Eclipse 50oi fluorescence microscope. Follicle counting was performed blindly on all sections per culture timepoint and per patient. gH2AX- and TUNEL-positive follicles (positive oocyte, one or more positive GCs or both cell types) were counted and reported as a percentage of the total number of follicles (positive and negative) per patient. KL staining was quantified on at least 30 (range: 30–98) primordial-primary follicles from at least three random sections per patient using ZEN 2.3 blue software (Carl Zeiss, Germany). CD31 and Sirius Red staining were quantified on whole sections using Image J software. Immunoblotting images were analyzed using Image J software, and protein levels were normalized on ACTIN (internal control) and the control protein level to allow comparison among conditions.

Gene expression analysis

RNA analyses were performed on isolated follicles using mechanical and enzymatic isolation protocols as previously described (Grosbois and Demeestere, 2018). Isolated follicles under 70 µm diameters were collected and rinsed twice in phosphate buffer before RNA extraction using RNAqueous-Micro Total RNA Isolation kit (Life Technologies, Belgium). Total RNA was quantified using a NanoDrop spectrophotometer (ThermoFisher, Belgium) and reverse transcribed using the GoScript Reverse Transcription Mix (Promega, Netherlands). Real-time quantitative PCR was then performed using the PowerTrack SYBR Green Master Mix (ThermoFisher, Belgium) on an Applied Biosystems QuantStudio 3 Real-Time PCR System. Samples were processed in triplicate for different target genes (*CCN2*, *BIRC1*, and *KL*) and normalized on hypoxanthine guanine phosphoribosyl transferase (*HPRT*) levels. Primers used were previously described (Grosbois and Demeestere, 2018). Gene expression levels were quantified using the cycle threshold (Ct) and $2^{-\Delta\Delta Ct}$ methods.

Statistical analysis

Considering the high inter-individual variability of human follicle distribution, the whole cohort was analyzed for individual parameters such as pubertal status, chemotherapeutic exposure, and pathology of the patient (Walker *et al.*, 2021). Experimental values were presented graphically with individual values and box plots. Means±standard deviation (SD) or median and interquartile range (IQR) were presented. Two-way repeated measures ANOVA was used to analyze experimental values according to chemotherapy exposure and time (D0 and D1). The interaction was tested in each model, and since no significant interaction was found, we focused on the main effect of chemotherapy exposure. Similarly, two-way repeated measures ANOVA was used to analyze the values according to pubertal status and time. For TUNEL and gH2AX analyses, we also performed separate analyses according to the time of last chemotherapy exposure (Δt chem-OTC; ≤1 month and ≥4 months) and the pathology (leukemia, medulloblastoma, and lymphoma) (Details of data according to subgroups are shown in the supplementary figures.). The normality of variables and the homogeneity of variances were verified with Shapiro–Wilk and Levene tests, respectively. The Mann–Whitney test was used as a non-parametric test to analyze data from cortical tissue according to the different variables. Statistical significance was considered as reached when the *P*-value was under 0.05. Statistical analyses were performed using IBM SPSS Statistics 25 and graphs were designed using Graphpad Prism 6 software.

Results

Population characteristics

The mean age of prepubertal (n = 8) and postpubertal patients (n = 8) was 5.75 ± 2.9 and 21.8 ± 5.56 years, respectively. In each age group, five patients had received a chemotherapy regimen before the cryopreservation procedure and three did not. The characteristics of the cohorts are reported in Supplementary Table SII.

Impact of previous chemotherapy exposure on stromal fibrosis and vascularization

To assess the direct impact of exposure to chemotherapy on the cortical tissue, we performed histological analyses on whole tissue at thawing (D0) and after 24 h culture (D1) (Fig. 1a and b). Collagen density appeared to be highly variable among the different patients, without age correlations (data not shown). At both culture timepoints, no differences in collagen density were observed between the postpubertal [D0: 62.95% (IQR 32.33%); D1: 40.10% (IQR 47.37%)] and prepubertal patients [D0: 66.72% (IQR 28.96%); D1: 48.05% (IQR 45.96%)] nor between the exposed [D0: 72.14% (IQR 20.23%); D1: 50.68% (IQR 32.91%)] and non-exposed groups [D0: 60.32% (IQR 52.26%); D1: 31.43% (IQR 56.38%)] (Fig. 1c; Supplementary Fig. S1a and b). Similarly, vascularization (CD31+ area) appeared stable among the pubertal groups (Supplementary Fig. S1c and d). However, the vascularization (CD31+) area was significantly lower at thawing in patients previously exposed to chemotherapy [0.61%; (IQR 0.59%)] compared to non-exposed patients [1.52% (IQR 1.19%)] ($P = 0.022$; Fig. 1d).

Effect of first exposure to chemotherapy on follicle survival

Follicular density (total follicle numbers per mm^2) was significantly higher in ovarian fragments from prepubertal patients (D0: 190.2 ± 184.5; D1: 129 ± 154.6) compared to postpubertal patients (D0: 22.2 ± 13.2; D1: 29.6 ± 25.1) ($P = 0.031$; Fig. 2a, Supplementary Fig. S2a). However the density did not vary according to the previous chemotherapy exposure ($P = 0.24$; Fig. 2b). Atretic follicles were counted according to their morphology and reported according to the total number of follicles. Atresia was observed at every follicle stage at

Downloaded from https://academic.oup.com/humrep/advance-article/doi/10.1093/humrep/dead013/7022048 by Universite Catholique de Louvain user on 08 February 2023

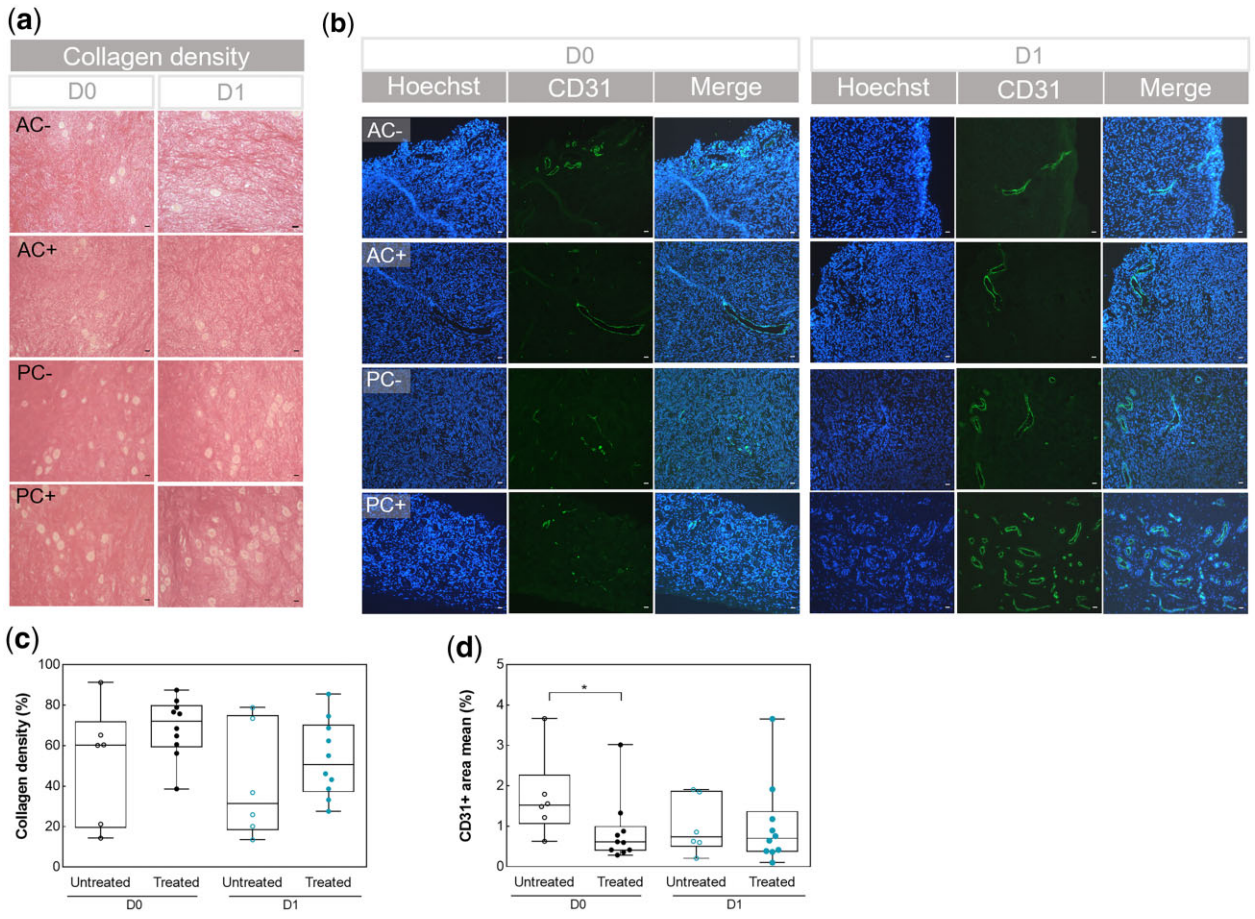

Figure 1. Stromal structure analyses. Cortical tissues were examined at thawing (D0) and after 1 day of culture (D1) and were from postpubertal (Post, A) and prepubertal (Pre, P) patients previously treated (C+) or not (C−) with chemotherapy. Picrosirius staining (**a**) and CD31 staining (**b**) images. Scale bar: 20 µm. (**c**) Quantification of collagen density into tissues of the different patient groups according to previous exposure to chemotherapy. (**d**) Quantification of CD31+ area into tissues of the different patient according to previous exposure to chemotherapy. Data are represented as median area and interquartile range (IQR) (*$P < 0.05$) (N = 16).

thawing and after culture (Supplementary Table SIII). Atresia rates were not significantly different between postpubertal and prepubertal patients ($P = 0.632$) nor between the exposed and non-exposed groups ($P = 0.922$) (Fig. 2c and d; Supplementary Fig. S2b and Supplementary Table SIII).

Apoptosis and the DDR were then evaluated by immunostaining (Fig. 3). The level of apoptosis measured using TUNEL staining was lower when the time between the last chemotherapy exposure and the OTC (Δt chem-OTC) was >4 months (D0: 8.93% ± 15.03%; D1: 15.62% ± 19.36%) ($P = 0.003$; Fig. 3b). Surprisingly, leukemic patients appeared to have a higher proportion of gH2AX-positive follicles (D0: 67.52% ± 34.39%; D1: 81.80% ± 16.45%), demonstrating high DDR induction, compared to non-leukemic patients (D0: 32.86% ± 23.38%; D1: 34.66% ± 22.18%) ($P = 0.008$; Fig. 3e). When excluding patients with leukemia or with Δt chem-OTC ≥4 months from the analysis to avoid bias, we confirmed that TUNEL staining was significantly higher in groups treated with chemotherapy compared to controls ($P < 0.001$; Fig. 3a and c), with no difference according to the pubertal status ($P = 0.886$; Supplementary Fig. S3a and b and Supplementary Table SIV). Both quiescent and activated follicles were subject to apoptosis, with a higher proportion of activated follicles being apoptotic in both groups (Supplementary Table SIV). At thawing, we observed more TUNEL-positive oocytes than GCs, while all cell types were stained at D1 (Supplementary Table SIV). Finally, the proportion of follicles positive for gH2AX was higher in the groups previously treated with chemotherapy compared to controls ($P = 0.043$; Fig. 3f), without variation according to the pubertal status ($P = 0.344$; Supplementary Fig. S3c and d).

Impact of chemotherapy exposure before OTC on follicle activation

Follicle activation was evaluated by follicle counting, immunostaining of PI3K and Hippo pathways proteins (KL, pAKT, pRPS6, and YAP), as

Downloaded from https://academic.oup.com/humrep/advance-article/doi/10.1093/humrep/dead013/7022048 by Universite Catholique de Louvain user on 08 February 2023

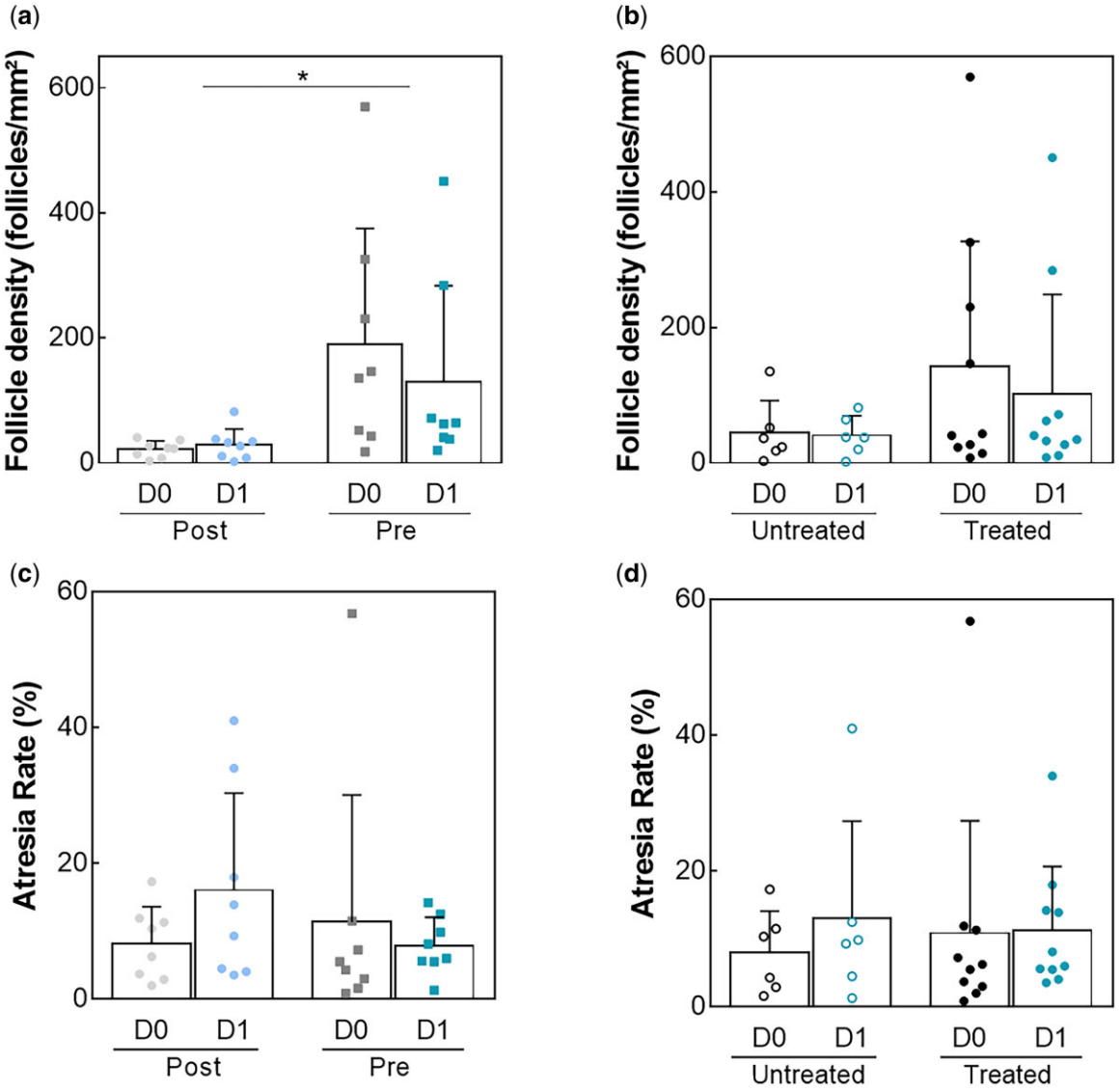

Figure 2. Follicle counting. Tissues were examined at thawing (D0) and after 24 h of culture (D1) and were from postpubertal (Post) and prepubertal (Pre) patients previously exposed or not to chemotherapy. Follicle density (mean of follicles per mm^2) among pubertal groups (**a**), and treatment groups (**b**). Atresia rate represented according to the pubertal status (**c**), and previous treatment (**d**). Data are represented as mean ± SD (N = 16 per timepoint) (*$P < 0.05$).

well as analyses of RNA, and protein expression of PI3K (*KL*, cKIT, AKT, pAKT, RPS6, pRPS6) and Hippo (*CCN2*, *BIRC1*, LATS1, YAP, and pYAP) signaling pathways. Follicular counting revealed no significant differences in the percentages of activated follicle between the pubertal groups at thawing and after 1 day in culture ($P = 0.656$; Supplementary Fig. S4a and b). A significant lower mean percentage of activated follicles was observed in the treated groups compared to the non-treated patients ($P = 0.015$; Fig. 4a). As KL is the major marker of induction of the PI3K signaling leading to activation of the follicle, we assessed *KL* gene expression in isolated follicles as well as protein expression in ovarian tissue. No significant differences in *KL* expression were observed according to previous chemotherapy exposure ($P = 0.735$; Fig. 4b, Supplementary Fig. S4c). Similarly, quantification of KL staining intensity per follicle ($P = 356$; Fig. 5a and b; Supplementary Fig. S5a) and cKIT protein level in whole tissue (data not shown) did not show any statistical difference among the patients at either timepoint of the analysis. We observed localization of pAKT in oocytes and a restriction to GCs for pRPS6, but no significant differences were reported in the signal intensity among the patients treated by chemotherapy before OTC or not (pAKT, $P = 0.878$; pRPS6, $P = 0.854$; Fig. 5a, c, and d; Supplementary Fig. S5b and c). Immunoblotting demonstrated similar expression of AKT, pAKT, and RPS6 protein level

Downloaded from https://academic.oup.com/humrep/advance-article/doi/10.1093/humrep/dead013/7022048 by Universite Catholique de Louvain user on 08 February 2023

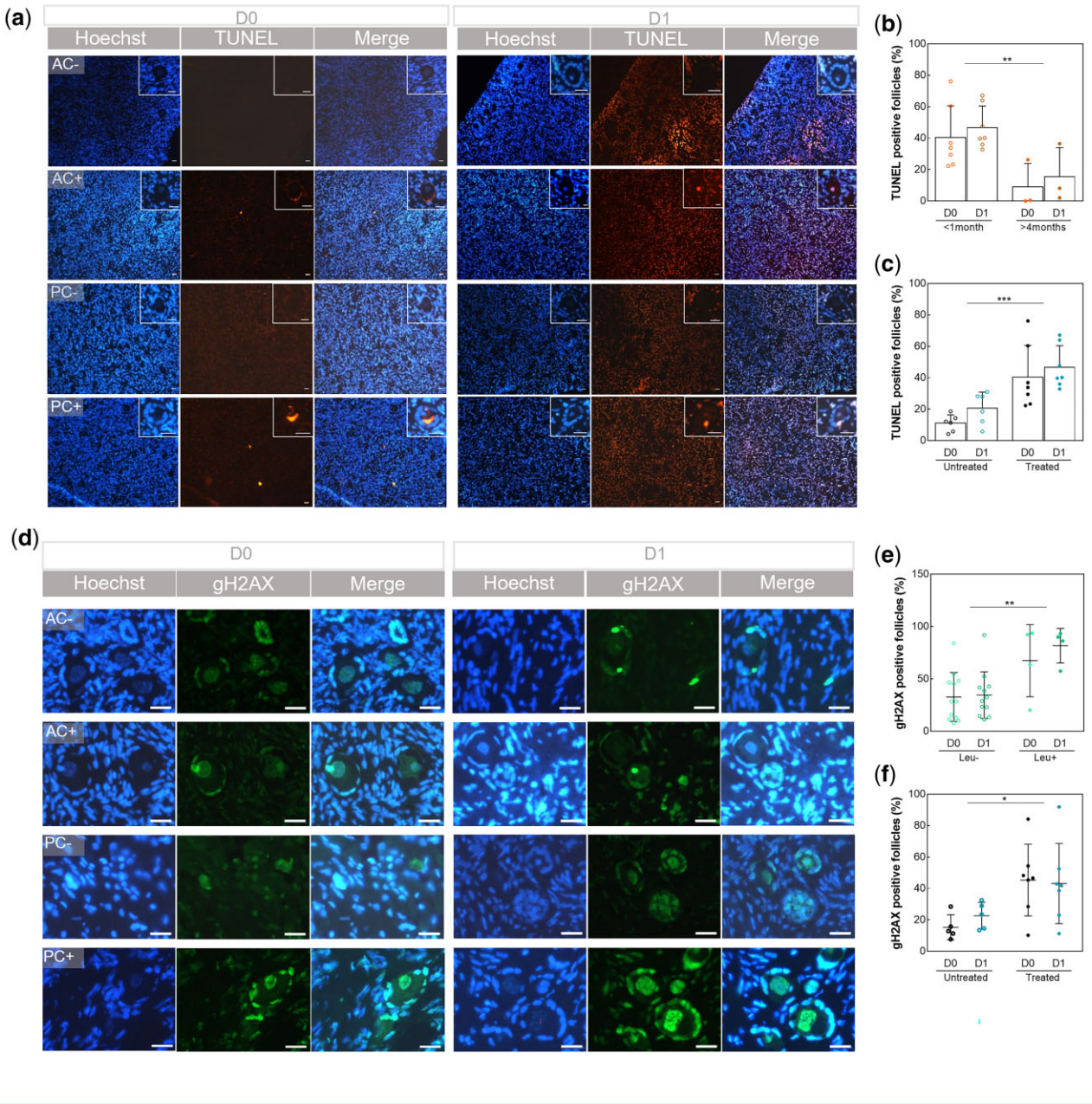

Figure 3. Follicle survival by time of analysis. Postpubertal (Post, A) and prepubertal (Pre, P) patients were previously exposed (C+) or not (C−) to chemotherapy. TUNEL staining images (**a**) and quantification of the follicles containing DNA damage among the different groups according to the time from the last chemotherapy exposure to ovarian tissue cryopreservation (**b**) (N = 16), and to the previous exposure to chemotherapy (**c**) (N = 13). gH2AX staining images (**d**) and quantification of the gH2AX-positive follicle rate according to the pathology (Leu, Leukemia) (N = 16) (**e**), and to the previous treatment (N = 12) (**f**). All values are mean percentage of follicles ± SD. Scale bar: 20 µm (*$P < 0.05$; **$P < 0.01$; ***$P < 0.001$).

among these patients (Fig. 5e and f) while pRPS6 levels were significantly higher in chemotherapy-treated patients compared to the non-treated patients at thawing ($P = 0.016$; Fig. 5e and g; Supplementary Fig. S6a–f).

Similarly, immunoblotting of Hippo pathway proteins showed a significant difference between the groups treated with chemotherapy compared to controls on LATS1 protein levels at thawing in the cortex ($P = 0.042$; Fig. 6a and b) but YAP and pYAP protein levels appeared to be stable among groups (Fig. 6a and c; Supplementary Fig. S7a–d). At the follicular level, immunostaining of YAP showed a restricted localization of the protein to the cytoplasm of GCs (Fig. 6d), supporting the absence of chemotherapy induced-disruption of the Hippo pathway in follicles. Finally, the expression of *CCN2* and *BIRC1* appeared to be stable in the follicles according to prior chemotherapy

Downloaded from https://academic.oup.com/humrep/advance-article/doi/10.1093/humrep/dead013/7022048 by Universite Catholique de Louvain user on 08 February 2023

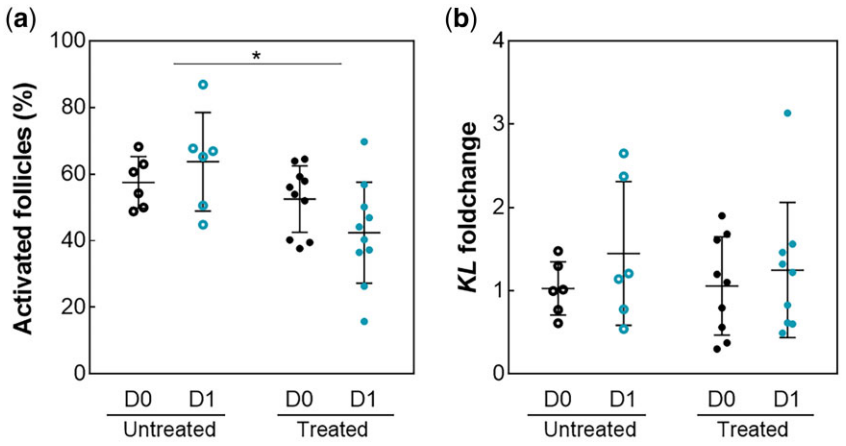

Figure 4. Impact of first chemotherapy exposure on follicle activation. Patients were previously treated or not treated by chemotherapy and tissues were examined at thawing (D0) and after 1 day of culture (D1). Mean percentage of activated follicles obtained after reporting healthy growing follicles (transitory, primary, secondary) as a proportion of the total number of follicles per patient (N = 16) (**a**). RNA expression of *KL* among untreated and treated patients (**b**). Levels were normalized on *HPRT* levels and the fold-change was obtained on the mean of each control group (N = 15). Data presented are mean with SD (*$P < 0.05$).

treatment or not at both culture timepoints (*CCN2*, $P = 0.546$; *BIRC1*, $P = 0.768$; Fig. 6e and f; Supplementary Fig. S7e and f).

Regarding the pubertal status, no difference was observed in the PI3K/AKT/mTOR and Hippo pathways proteins analyzed, except for the YAP level showing higher expression in the cortex of prepubertal patients [1.20 (IQR 1.01)] compared to postpubertal patients [0.72 (IQR 0.22)] after 24 h of culture ($P = 0.015$) (data not shown).

Discussion

Although the gonadotoxic effects of chemotherapy exposure are well established, the mechanisms leading to follicle depletion are still not clear, particularly in humans. Individual characteristics of the patients, the disease, and the exposure to multidrug therapies have introduced multiple possible sources of bias that have complicated these analyses. Moreover, some patients receive a chemotherapy regimen before the OTC procedure, which may impact further establishment of an appropriate and reliable human follicle culture system (Ghezelayagh *et al.*, 2022).

In this study, different parameters including fibrosis, vascularization, follicular death, and follicular activation were assessed according to pubertal status and prior chemotherapy exposure. Stromal and vascular damages have been reported after chemotherapy exposure in human ovarian tissue (Meirow *et al.*, 2007; Pampanini *et al.*, 2019; Shai *et al.*, 2021). In this study, significant differences in collagen density were not observed between the patients previously treated with chemotherapy compared to controls, irrespective of age or time of culture. The absence of an effect of chemotherapy exposure on fibrosis in our cohort could be due to the short time between exposure and OTC, as fibrosis is usually observed 4–6 months after the exposure (Shai *et al.*, 2021). In contrast, a decrease in vessel area was observed in the tissue from patients previously treated with chemotherapy compared to that from non-exposed patients at thawing. Although PFs are known to be unaffected by perfusion, the impairment of vessel integrity following chemotherapy-exposure could increase tissue ischemia following OTC. This altered microenvironment could negatively impact the ovarian pool and should be further investigated (Soleimani *et al.*, 2011). The major gonadotoxic effects of chemotherapy exposure include double-strand breaks (DSBs) and DNA replication disruption (Bedoschi *et al.*, 2016). Depending on the chemotherapeutic agent, the dose, and the model studied, the direct impact on PFs appears to be variable (Spears *et al.*, 2019). After CPA exposure, *in vivo* mouse experiments did not demonstrate apoptosis in PFs, while xenografting experiments using human ovarian tissue showed the presence of DNA damage in PFs (Kalich-Philosoph *et al.*, 2013; Titus *et al.*, 2021). Anthracycline agents, such as doxorubicin (DOX), have been reported to induce DNA DSBs into PF oocytes and GCs, as well as vessel and stromal damage (Soleimani *et al.*, 2011; Morgan *et al.*, 2013; Lopes *et al.*, 2019). However, regimens including DOX, such as the DOX–bleomycin–vinblastine–dacarbazine (ABVD) regimen for lymphoma, are considered to be low risk for POI while platinum agents cause specific apoptosis induction following DSBs in oocytes (Morgan *et al.*, 2013; Spears *et al.*, 2019; Allen *et al.*, 2020; Nguyen *et al.*, 2021). Oncological treatments usually include multiple chemotherapeutic agents and new drugs are constantly being developed, making fertility counseling complex. In this study, we could not avoid the high heterogeneity of patients and treatments reflecting the clinical reality. For that reason, our study included 10 patients previously treated with different chemotherapy regimens. All patients except two received alkylating agents in the treatment administered, but we did not observe any difference in follicular damage between treated patients. When we compared treated with untreated patients, the atretic follicle rates were similar as was as the follicular density, but the TUNEL staining analyses sustained a transient deleterious impact of chemotherapy exposure on

Downloaded from https://academic.oup.com/humrep/advance-article/doi/10.1093/humrep/dead013/7022048 by Universite Catholique de Louvain user on 08 February 2023

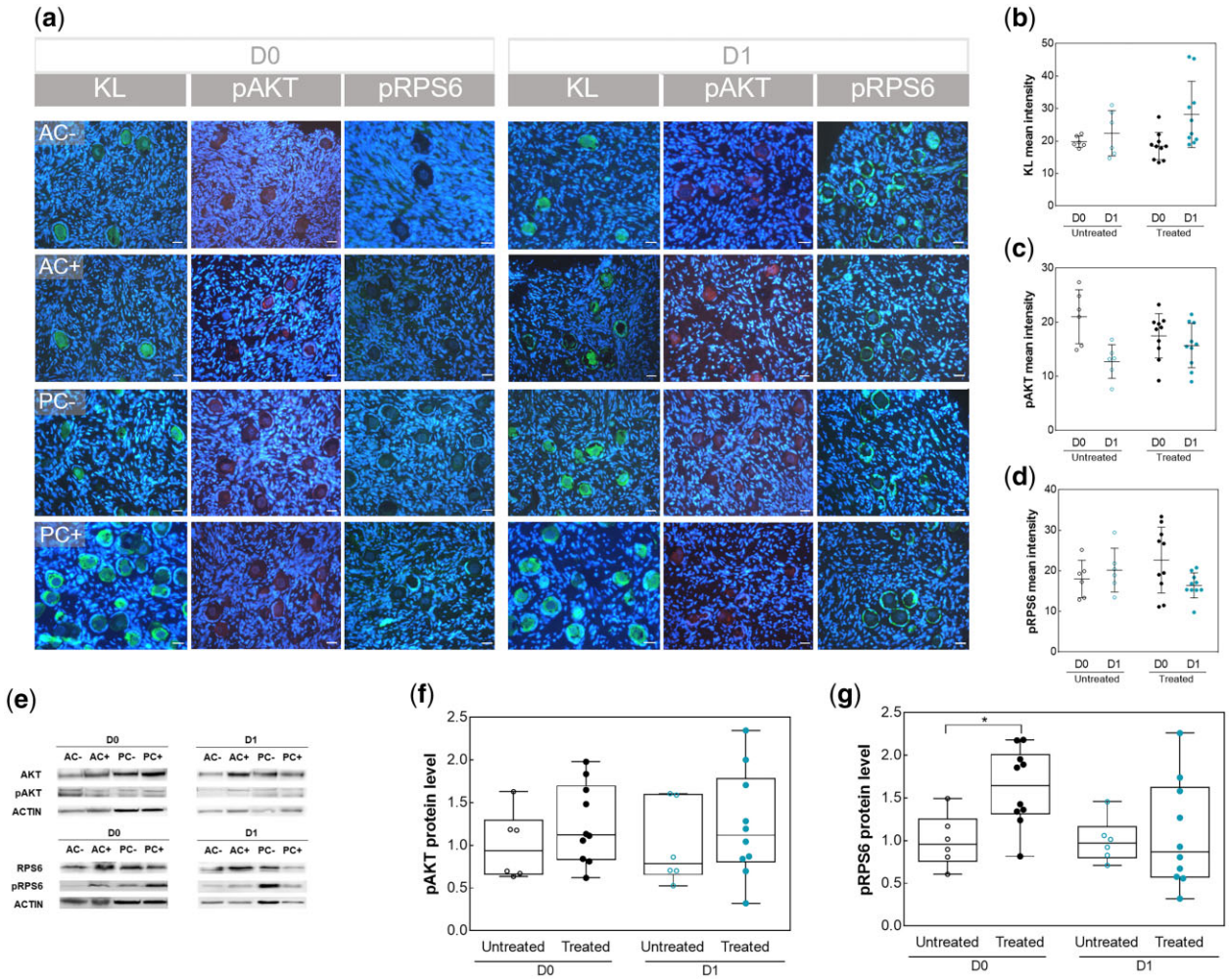

Figure 5. Impact of first chemotherapy exposure on the PI3K pathway. Postpubertal (Post, A) and prepubertal (Pre, P) patients were grouped according to the presence (C+) or absence (C−) of a previous chemotherapeutic treatment. (**a**) Images of immunostaining on KL, pAKT, and pRPS6. Scale bar: 20 µm. Quantification of KL (**b**), pAKT (**c**), and pRPS6 (**d**) intensity staining per follicle among the patients according to previous treatment or not. Bars represent the mean of signal intensity with SD. (**e**) Western blot on AKT, RPS6, pAKT, and pRPS6. Quantification of the activated protein levels of pAKT (**f**) and pRPS6 (**g**) among groups. All values were normalized on actin levels and on the mean of each control group, values are median ± IQR (*$P < 0.05$) (N = 16).

follicle survival. We observed that the apoptosis rate was decreased with time since exposure, indicating an acute effect of chemotherapy on follicle survival, consistent with a previous report (Shai *et al.*, 2021). Overall, growing follicles were more sensitive to chemotherapy-induced death while quiescent follicles were also affected, as previously reported (Kalich-Philosoph *et al.*, 2013; Titus *et al.*, 2021).

Surprisingly, our analyses revealed a significantly higher DDR induction in the four leukemic patients compared to that in the other patients. All of the leukemic patients involved in our study were acute lymphoblastic leukemia (ALL). Phosphorylation of H2AX (gH2AX) is an early marker of DSBs indicating the initiation of DNA repair mechanisms (Ismail and Hendzel, 2008). Studies in cells have demonstrated higher gH2AX rates in the presence of BCR-ABL or histone methyltransferase enhancer of zeste homolog 2 protein (EHZ2) mutations, two reported mutations involved in the ALL etiology, compared to controls (Wu *et al.*, 2011; Schäfer *et al.*, 2016; Popp *et al.*, 2020). Unfortunately, the genetic profile of our patients was not available to support this possible association in our model. To our knowledge, this is the first report of a potential link between ALL and high H2AX phosphorylation rates in the ovarian follicle, raising awareness of the possible impact of the mutation of these genes on the DDR mechanisms in ovarian follicles. Consistent with the TUNEL analyses, the chemotherapy-treated patients overall in this study had a higher proportion of gH2AX-positive follicles compared to non-exposed patients. Recently, Oktay *et al.* reported differential expression of DNA repair genes in adults and children (Oktay *et al.*, 2022). This study suggested that postpubertal and prepubertal patients

Downloaded from https://academic.oup.com/humrep/advance-article/doi/10.1093/humrep/dead013/7022048 by Universite Catholique de Louvain user on 08 February 2023

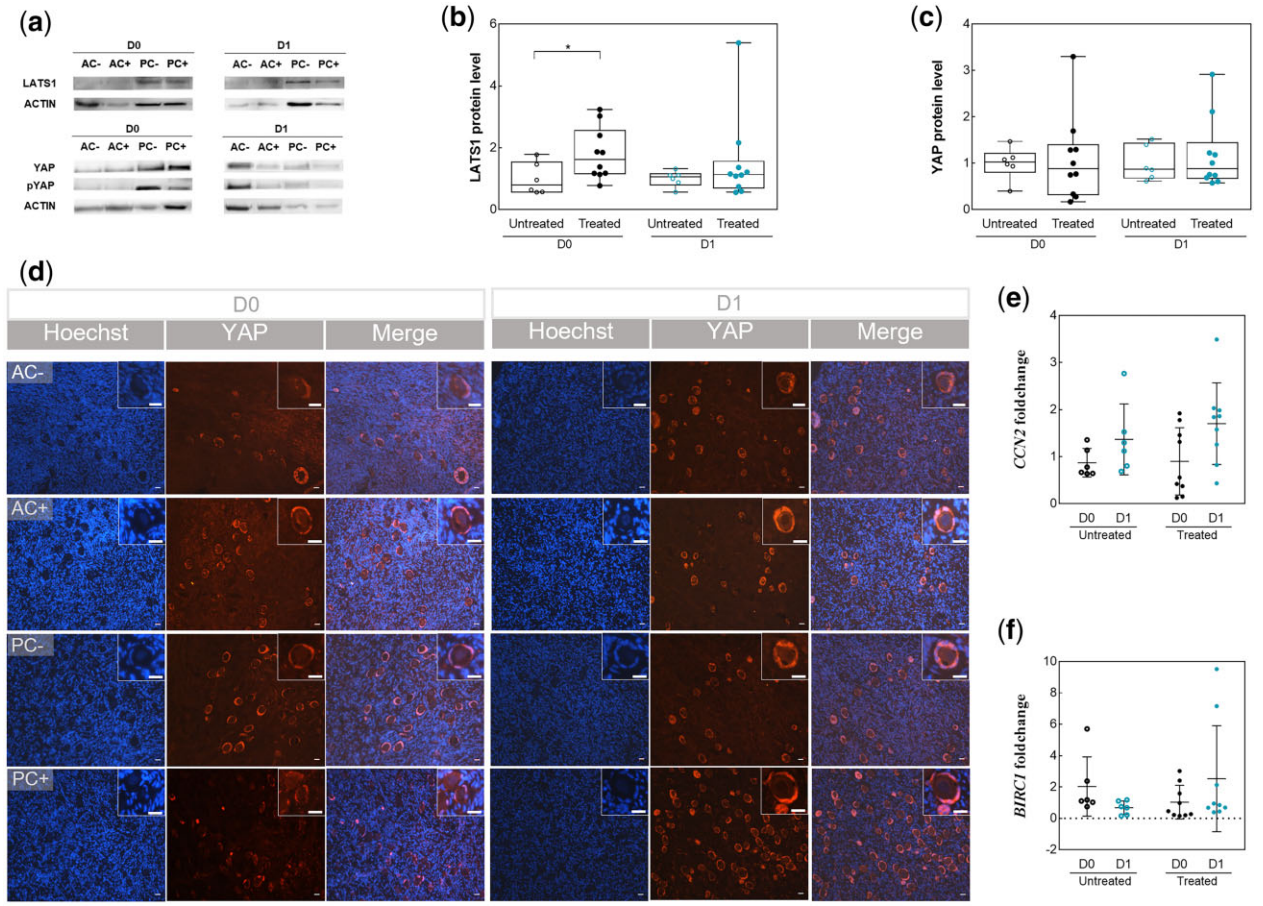

Figure 6. Impact of chemotherapy exposure on the Hippo signaling pathway. Tissues were from postpubertal (Post, A) and prepubertal (Pre, P) patients previously treated (C+) or not (C−) by chemotherapy. (**a**) Western blot on LATS1, YAP, and pYAP. Quantification of LATS1 (**b**) and YAP (**c**) protein levels among the patients according to previous treatment or not. All values were normalized on ACTIN level and on the control mean of each group, values are median and IQR (N = 16). (**d**) Images of immunostaining on YAP. Scale bar = 20 µm. RNA expression of *CCN2* (**e**) and *BIRC1* (**f**) among the different treatment groups. Levels were normalized on *HPRT* levels and fold-change was obtained on the mean of each control group (N = 15). Data presented are mean fold-change with SD (*$P < 0.05$).

do not have the same ability to respond to DNA damage, and therefore, the subsequent number of follicles with DNA repairs may vary. In our study, we did not demonstrate different cellular responses to DSBs according to pubertal status.

Several studies assessing the impact of chemotherapy on ovarian tissue have reported increased follicular activation, leading to the depletion of the ovarian stockpile (Kalich-Philosoph *et al.*, 2013; Lande *et al.*, 2017; Shai *et al.*, 2021). This 'burn-out' effect has been challenged by other studies which have demonstrated that the follicular depletion is related to an apoptotic process rather than activation (Luan *et al.*, 2019; Pampanini *et al.*, 2019). Our study showed a decrease in the proportion of growing follicles in patients who were treated with chemotherapy, supporting the absence of chemotherapy-induced follicle activation. No significant differences were observed in KL gene and protein expression, cKIT protein levels or AKT phosphorylation rates among the patients in this study. However, an increase in activation of RPS6 was observed in treated patients, indicating an induction of the mTOR pathway in the cortical tissue. Regarding the Hippo pathway, our analyses showed no impact on the main effectors expression such as *CCN2* in the follicles, while it revealed a significant higher LATS1 protein level at thawing in treated tissue after whole cortex analysis. The potential indirect impact of these changes in PI3K and Hippo pathways in the cortex on the follicular activation and survival require further investigation. The Hippo pathway component has been reported to interact with other signaling including angiogenesis processes (Tsuneki and Madri, 2014; Boopathy and Hong, 2019). We observed here a lower vascularization (CD31+) area in patients treated with chemotherapy compared to untreated patients, but its relation to a potential disruption of the Hippo pathway should be further confirmed.

In conclusion, our results suggest that chemotherapy exposure prior to OTC induces acute DNA damage in follicles rather than massive

Downloaded from https://academic.oup.com/humrep/advance-article/doi/10.1093/humrep/dead013/7022048 by Universite Catholique de Louvain user on 08 February 2023

activation. However, a possible additional impact on endothelial structures, and on the mTOR and Hippo pathways in the whole cortex, was observed in exposed patients, with potential long-term consequences on follicular development. Finally, our data indicate that the underlying pathology of the patient could also affect the DDR mechanisms in the ovarian follicle. The limited number of included patients, as well as the heterogeneity of the treatments are important limitations to our study. Further investigation is needed to better understand chemotherapy-induced alterations in human ovary tissue.

Supplementary data

Supplementary data are available at *Human Reproduction* online.

Data availability

The data presented in this manuscript can be shared on request to the corresponding authors.

Authors' roles

I.D. designed the study. M.D. performed experiments and analyzed the data. P.D.V. performed the tissue processing. E.A. and M.-M.D. contributed to the inclusion of patients. J.B. contributed to the statistical analyses. M.D. and I.D. wrote the manuscript. All authors contributed to the data interpretation and gave approval of the manuscript.

Funding

This study was funded by an Excellence of Science (EOS) Grant (ID: 30443682) and was supported by Fonds Erasme.

Conflict of interest

The authors have no conflict of interest to declare related to this work.

References

Adhikari D, Zheng W, Shen Y, Gorre N, Hamalainen T, Cooney AJ, Huhtaniemi I, Lan Z-J, Liu K. Tsc/mTORC1 signaling in oocytes governs the quiescence and activation of primordial follicles. *Hum Mol Genet* 2010;**19**:397–410.

Allen CM, Lopes F, Mitchell RT, Spears N. Comparative gonadotoxicity of the chemotherapy drugs cisplatin and carboplatin on prepubertal mouse gonads. *Mol Hum Reprod* 2020;**26**:129–140.

Bedoschi G, Navarro PA, Oktay K. Chemotherapy-induced damage to ovary: mechanisms and clinical impact. *Future Oncol* 2016;**12**:2333–2344.

Ben-Aharon I, Shalgi R. What lies behind chemotherapy-induced ovarian toxicity? *Reproduction* 2012;**144**:153–163.

Boopathy GTK, Hong W. Role of Hippo pathway-YAP/TAZ signaling in angiogenesis. *Front Cell Dev Biol* 2019;**7**:49.

Castrillon DH, Miao L, Kollipara R, Horner JW, DePinho RA. Suppression of ovarian follicle activation in mice by the transcription factor Foxo3a. *Science* 2003;**301**:215–218.

Chen X-Y, Xia H-X, Guan H-Y, Li B, Zhang W. Follicle loss and apoptosis in cyclophosphamide-treated mice: what's the matter? *Int J Mol Sci* 2016;**17**:836.

Chiarelli AM, Marrett LD, Darlington G. Early menopause and infertility in females after treatment for childhood cancer diagnosed in 1964–1988 in Ontario, Canada. *Am J Epidemiol* 1999;**150**:245–254.

Couzens AL, Xiong S, Knight JDR, Mao DY, Guettler S, Picaud S, Kurinov I, Filippakopoulos P, Sicheri F, Gingras A-C. MOB1 mediated phospho-recognition in the core mammalian Hippo pathway. *Mol Cell Proteomics* 2017;**16**:1098–1110.

Demeestere I, Simon P, Buxant F, Robin V, Fernandez SA, Centner J, Delbaere A, Englert Y. Ovarian function and spontaneous pregnancy after combined heterotopic and orthotopic cryopreserved ovarian tissue transplantation in a patient previously treated with bone marrow transplantation: case report. *Hum Reprod* 2006;**21**:2010–2014.

Demeestere I, Simon P, Englert Y, Delbaere A. Preliminary experience of ovarian tissue cryopreservation procedure: alternatives, perspectives and feasibility. *Reprod Biomed Online* 2003;**7**:572–579.

Devos M, Grosbois J, Demeestere I. Interaction between PI3K/AKT and Hippo pathways during in vitro follicular activation and response to fragmentation and chemotherapy exposure using a mouse immature ovary model. *Biol Reprod* 2020;**102**:717–729.

Dinikina Y, Belogurova M, Zaritskey A, Govorov I, Tsibizova V, Gamzatova Z, Pervunina T, Komlichenko E. Ovarian tissue cryopreservation in prepubertal patients with oncological diseases: multidisciplinary approach and outcomes. *J Matern Fetal Neonatal Med* 2021;**34**:2391–2398.

Driancourt MA, Reynaud K, Cortvrindt R, Smitz J. Roles of KIT and KIT LIGAND in ovarian function. *Rev Reprod* 2000;**5**:143–152.

ESHRE Guideline Group on Female Fertility Preservation; Anderson RA, Amant F, Braat D, D'Angelo A, Chuva de Sousa Lopes SM, Demeestere I, Dwek S, Frith L, Lambertini M, Maslin C *et al.* ESHRE guideline: female fertility preservation. *Hum Reprod Open* 2020;**2020**:hoaa052.

Filippi F, Meazza C, Somigliana E, Podda M, Dallagiovanna C, Massimino M, Raspagliesi F, Terenziani M. Fertility preservation in childhood and adolescent female tumor survivors. *Fertil Steril* 2021;**116**:1087–1095.

Ghezelayagh Z, Khoshdel-Rad N, Ebrahimi B. Human ovarian tissue in-vitro culture: primordial follicle activation as a new strategy for female fertility preservation. *Cytotechnology* 2022;**74**:1–15.

Grosbois J, Demeestere I. Dynamics of PI3K and Hippo signaling pathways during in vitro human follicle activation. *Hum Reprod* 2018;**33**:1705–1714.

Grosbois J, Devos M, Demeestere I. Implications of nonphysiological ovarian primordial follicle activation for fertility preservation. *Endocrine Rev* 2020;**41**:847–872.

Guo Z, Yu Q. Role of mTOR signaling in female reproduction. *Front Endocrinol (Lausanne)* 2019;**10**:692.

Harvey KF, Zhang X, Thomas DM. The Hippo pathway and human cancer. *Nat Rev Cancer* 2013;**13**:246–257.

Hsueh AJW. Fertility: the role of mTOR signaling and KIT ligand. *Curr Biol* 2014;**24**:R1040–R1042.

Huang J, Dibble CC, Matsuzaki M, Manning BD. The TSC1-TSC2 complex is required for proper activation of mTOR complex 2. *Mol Cell Biol* 2008;**28**:4104–4115.

Downloaded from https://academic.oup.com/humrep/advance-article/doi/10.1093/humrep/dead013/7022048 by Universite Catholique de Louvain user on 08 February 2023

Ismail IH, Hendzel MJ. The gamma-H2A.X: is it just a surrogate marker of double-strand breaks or much more? *Environ Mol Mutagen* 2008;**49**:73–82.

Jensen AK, Rechnitzer C, Macklon KT, Ifversen MRS, Birkebæk N, Clausen N, Sørensen K, Fedder J, Ernst E, Andersen CY. Cryopreservation of ovarian tissue for fertility preservation in a large cohort of young girls: focus on pubertal development. *Hum Reprod* 2017;**32**:154–164.

John GB, Gallardo TD, Shirley LJ, Castrillon DH. Foxo3 is a PI3K-dependent molecular switch controlling the initiation of oocyte growth. *Dev Biol* 2008;**321**:197–204.

Kalich-Philosoph L, Roness H, Carmely A, Fishel-Bartal M, Ligumsky H, Paglin S, Wolf I, Kanety H, Sredni B, Meirow D. Cyclophosphamide triggers follicle activation and "burnout"; AS101 prevents follicle loss and preserves fertility. *Sci Transl Med* 2013;**5**:185ra62.

Kano M, Sosulski AE, Zhang L, Saatcioglu HD, Wang D, Nagykery N, Sabatini ME, Gao G, Donahoe PK, Pépin D. AMH/MIS as a contraceptive that protects the ovarian reserve during chemotherapy. *Proc Natl Acad Sci U S A* 2017;**114**:E1688–E1697.

Kawamura K, Cheng Y, Suzuki N, Deguchi M, Sato Y, Takae S, Ho C-H, Kawamura N, Tamura M, Hashimoto S *et al.* Hippo signaling disruption and Akt stimulation of ovarian follicles for infertility treatment. *Proc Natl Acad Sci U S A* 2013;**110**:17474–17479.

Lambertini M, Peccatori FA, Demeestere I, Amant F, Wyns C, Stukenborg J-B, Paluch-Shimon S, Halaska MJ, Uzan C, Meissner J *et al.*; ESMO Guidelines Committee. Fertility preservation and post-treatment pregnancies in post-pubertal cancer patients: ESMO Clinical Practice Guidelines. *Ann Oncol* 2020;**31**:1664–1678.

Lande Y, Fisch B, Tsur A, Farhi J, Prag-Rosenberg R, Ben-Haroush A, Kessler-Icekson G, Zahalka MA, Ludeman SM, Abir R. Short-term exposure of human ovarian follicles to cyclophosphamide metabolites seems to promote follicular activation in vitro. *Reprod Biomed Online* 2017;**34**:104–114.

Lopes F, Liu J, Morgan S, Matthews R, Nevin L, Anderson RA, Spears N. Single and combined effects of cisplatin and doxorubicin on the human and mouse ovary in vitro. *Reproduction* 2020;**159**:193–204.

Luan Y, Edmonds ME, Woodruff TK, Kim S-Y. Inhibitors of apoptosis protect the ovarian reserve from cyclophosphamide. *J Endocrinol* 2019;**240**:243–256.

Lunding SA, Andersen AN, Hardardottir L, Olesen HØ, Kristensen SG, Andersen CY, Pors SE. Hippo signaling, actin polymerization, and follicle activation in fragmented human ovarian cortex. *Mol Reprod Dev* 2020;**87**:711–719.

Mamane Y, Petroulakis E, Rong L, Yoshida K, Ler LW, Sonenberg N. eIF4E–from translation to transformation. *Oncogene* 2004;**23**:3172–3179.

Manning BD, Cantley LC. AKT/PKB signaling: navigating downstream. *Cell* 2007;**129**:1261–1274.

McLaughlin M, Albertini DF, Wallace WHB, Anderson RA, Telfer EE. Metaphase II oocytes from human unilaminar follicles grown in a multi-step culture system. *Mol Hum Reprod* 2018;**24**:135–142.

McLaughlin M, Kelsey TW, Wallace WHB, Anderson RA, Telfer EE. Non-growing follicle density is increased following adriamycin, bleomycin, vinblastine and dacarbazine (ABVD) chemotherapy in the adult human ovary. *Hum Reprod* 2017;**32**:165–174.

Meirow D. Reproduction post-chemotherapy in young cancer patients. *Mol Cell Endocrinol* 2000;**169**:123–131.

Meirow D, Biederman H, Anderson RA, Wallace WHB. Toxicity of chemotherapy and radiation on female reproduction. *Clin Obstet Gynecol* 2010;**53**:727–739.

Meirow D, Dor J, Kaufman B, Shrim A, Rabinovici J, Schiff E, Raanani H, Levron J, Fridman E. Cortical fibrosis and blood-vessels damage in human ovaries exposed to chemotherapy. Potential mechanisms of ovarian injury. *Hum Reprod* 2007;**22**:1626–1633.

Morgan S, Lopes F, Gourley C, Anderson RA, Spears N. Cisplatin and doxorubicin induce distinct mechanisms of ovarian follicle loss; imatinib provides selective protection only against cisplatin. *PLoS One* 2013;**8**:e70117.

Mulder RL, Font-Gonzalez A, Hudson MM, van Santen HM, Loeffen EAH, Burns KC, Quinn GP, van Dulmen-den Broeder E, Byrne J, Haupt R *et al.* Fertility preservation for female patients with childhood, adolescent, and young adult cancer: recommendations from the PanCareLIFE Consortium and the International Late Effects of Childhood Cancer Guideline Harmonization Group. *Lancet Oncol* 2021;**22**:e45–e56.

Nguyen Q-N, Zerafa N, Findlay JK, Hickey M, Hutt KJ. DNA repair in primordial follicle oocytes following cisplatin treatment. *J Assist Reprod Genet* 2021;**38**:1405–1417.

Nicosia SV, Matus-Ridley M, Meadows AT. Gonadal effects of cancer therapy in girls. *Cancer* 1985;**55**:2364–2372.

Oktay KH, Marin L, Titus S. Impact of chemotherapy on the ovarian reserve: are all primordial follicles created equal? *Fertil Steril* 2022;**117**:396–398.

Oktem O, Oktay K. A novel ovarian xenografting model to characterize the impact of chemotherapy agents on human primordial follicle reserve. *Cancer Res* 2007;**67**:10159–10162.

Pampanini V, Wagner M, Asadi-Azarbaijani B, Oskam IC, Sheikhi M, Sjödin MOD, Lindberg J, Hovatta O, Sahlin L, Björvang RD *et al.* Impact of first-line cancer treatment on the follicle quality in cryopreserved ovarian samples from girls and young women. *Hum Reprod* 2019;**34**:1674–1685.

Popp HD, Kohl V, Naumann N, Flach J, Brendel S, Kleiner H, Weiss C, Seifarth W, Saussele S, Hofmann W-K *et al.* DNA damage and DNA damage response in chronic myeloid leukemia. *Int J Mol Sci* 2020;**21**:1177.

Schäfer V, Ernst J, Rinke J, Winkelmann N, Beck JF, Hochhaus A, Gruhn B, Ernst T. EZH2 mutations and promoter hypermethylation in childhood acute lymphoblastic leukemia. *J Cancer Res Clin Oncol* 2016;**142**:1641–1650.

Shai D, Aviel-Ronen S, Spector I, Raanani H, Shapira M, Gat I, Roness H, Meirow D. Ovaries of patients recently treated with alkylating agent chemotherapy indicate the presence of acute follicle activation, elucidating its role among other proposed mechanisms of follicle loss. *Fertil Steril* 2021;**115**:1239–1249.

Soleimani R, Heytens E, Darzynkiewicz Z, Oktay K. Mechanisms of chemotherapy-induced human ovarian aging: double strand DNA breaks and microvascular compromise. *Aging (Albany NY)* 2011;**3**:782–793.

Spears N, Lopes F, Stefansdottir A, Rossi V, De Felici M, Anderson RA, Klinger FG. Ovarian damage from chemotherapy and current approaches to its protection. *Hum Reprod Update* 2019;**25**:673–693.

Downloaded from https://academic.oup.com/humrep/advance-article/doi/10.1093/humrep/dead013/7022048 by Universite Catholique de Louvain user on 08 February 2023

Szymanska KJ, Tan X, Oktay K. Unraveling the mechanisms of chemotherapy-induced damage to human primordial follicle reserve: road to developing therapeutics for fertility preservation and reversing ovarian aging. *Mol Hum Reprod* 2020;**26**:553–566.

Titus S, Szymanska KJ, Musul B, Turan V, Taylan E, Garcia-Milian R, Mehta S, Oktay K. Individual-oocyte transcriptomic analysis shows that genotoxic chemotherapy depletes human primordial follicle reserve in vivo by triggering proapoptotic pathways without growth activation. *Sci Rep* 2021;**11**:407.

Tsuneki M, Madri JA. Adhesion molecule-mediated hippo pathway modulates hemangioendothelioma cell behavior. *Mol Cell Biol* 2014;**34**:4485–4499.

Walker CA, Bjarkadottir BD, Fatum M, Lane S, Williams SA. Variation in follicle health and development in cultured cryopreserved ovarian cortical tissue: a study of ovarian tissue from patients undergoing fertility preservation. *Hum Fertil (Camb)* 2021;**24**:188–198.

Wu Z, Lee ST, Qiao Y, Li Z, Lee PL, Lee YJ, Jiang X, Tan J, Aau M, Lim CZH *et al.* Polycomb protein EZH2 regulates cancer cell fate decision in response to DNA damage. *Cell Death Differ* 2011;**18**: 1771–1779.

Zhou D, Conrad C, Xia F, Park J-S, Payer B, Yin Y, Lauwers GY, Thasler W, Lee JT, Avruch J *et al.* Mst1 and Mst2 maintain hepatocyte quiescence and suppress hepatocellular carcinoma development through inactivation of the Yap1 oncogene. *Cancer Cell* 2009; **16**:425–438.

Zygulska AL, Krzemieniecki K, Pierzchalski P. Hippo pathway – brief overview of its relevance in cancer. *J Physiol Pharmacol* 2017;**68**: 311–335.

Downloaded from https://academic.oup.com/humrep/advance-article/doi/10.1093/humrep/dead013/7022048 by Universite Catholique de Louvain user on 08 February 2023